Letter

Kinetic approach of light-nuclei production in intermediate-energy heavy-ion collisions

Rui Wang [1,2,*] Yu-Gang Ma [1,3,†] Lie-Wen Chen [4,‡] Che Ming Ko [5,§] Kai-Jia Sun,[1,3,‖] and Zhen Zhang [6,¶]

[1] *Key Laboratory of Nuclear Physics and Ion-beam Application (MOE), and Institute of Modern Physics, Fudan University, Shanghai 200433, China*
[2] *Shanghai Institute of Applied Physics, Chinese Academy of Sciences, Shanghai 201800, China*
[3] *Shanghai Research Center for Theoretical Nuclear Physics (NSFC), Fudan University, Shanghai 200438, China*
[4] *School of Physics and Astronomy, Shanghai Key Laboratory for Particle Physics and Cosmology, and Key Laboratory for Particle Astrophysics and Cosmology (MOE), Shanghai Jiao Tong University, Shanghai 200240, China*
[5] *Cyclotron Institute and Department of Physics and Astronomy, Texas A&M University, College Station, Texas 77843, USA*
[6] *Sino-French Institute of Nuclear Engineering and Technology, Sun Yat-Sen University, Zhuhai 519082, China*

(Received 11 February 2023; accepted 29 August 2023; published 22 September 2023)

We develop a kinetic approach to the production of light nuclei up to mass number $A \leqslant 4$ in intermediate-energy heavy-ion collisions by including them as dynamic degrees of freedom. The conversions between nucleons and light nuclei during the collisions are incorporated dynamically via the breakup of light nuclei by a nucleon and their reverse reactions. We also include the Mott effect on light nuclei; i.e., a light nucleus will no longer be bound if the phase-space density of its surrounding nucleons is too large. With this kinetic approach, we obtain a reasonable description of the measured yields of light nuclei in central Au + Au collisions at energies of 0.25*A* GeV–1.0*A* GeV by the FOPI Collaboration. Our study also indicates that the observed enhancement of the α-particle yield at low incident energies can be attributed to a weaker Mott effect on the α particle, which makes it more difficult to dissolve in nuclear medium, as a result of its much larger binding energy.

DOI: 10.1103/PhysRevC.108.L031601

Heavy-ion collisions from the Fermi energy to the GeV region have been extensively used to study the properties of nucleon-nucleon effective interactions and the nuclear equation of state [1,2]. Significant progress has been achieved from studying in these collisions the nucleon and pion observables, such as the proton collective flow [3], the neutron-to-proton spectral ratio [4], and the charged pion ratio [5,6]. Since light nuclei are abundantly produced in heavy-ion collisions in this energy region, they are expected to have significant effects on the collision dynamics, which can then influence the nucleon and pion observables [7]. Therefore, a reliable theoretical description of these collisions requires treating light nuclei on the same footing as nucleons and pions. In this case, these collisions can also provide the possibility to study the in-medium properties of light nuclei and their fraction in warm nuclear matter [8–10], which are known to have important implications for the dynamics of core-collapse supernovas, as well as for the properties of compact stars and their mergers [11,12].

Despite their great importance, light-nuclei observables in heavy-ion collisions have not received as much attention as the nucleon and pion observables, and they are also not explicitly included in most theoretical approaches for heavy-ion collisions. Although there were attempts to describe light nuclei dynamically in transport models [13–15], the α particle was not included in these studies. Since then, new measurements of light nuclei up to mass number $A \leqslant 4$ in heavy-ion collisions from the Fermi energy to the GeV region, especially for Au + Au collisions, have become available from the INDRA and FOPI Collaborations [16,17]. The measured data show a significantly enhanced yield of the α particle in collisions at low incident energies. This surprising result has been suggested as an evidence for the Mott effect of light nuclei [9]; i.e., a light nucleus will no longer be bound if the phase-space density of its surrounding nucleons is too large [18,19]. These new measurements call for a dynamical approach for these collisions that includes all light nuclei up to the α particle.

In the present study, based on the real-time many-body Green's function formalism [20], we develop a kinetic approach to intermediate-energy heavy-ion collisions by including both nucleon and light-nuclei ($A \leqslant 4$) degrees of freedom. Specifically, the production and dissociation of the deuteron (d), triton (t), helium-3 (h), and α particle appear in this formalism as many-particle scatterings. The Mott effects on these nuclei are also included explicitly by considering the nucleon phase-space density around them. With this kinetic approach, we are able to reproduce the measured light-nuclei yields in central Au + Au collision at energies of 0.25*A* GeV–1.0*A* GeV by the FOPI Collaboration. We further show that

*wangrui@sinap.ac.cn
†mayugang@fudan.edu.cn
‡lwchen@sjtu.edu.cn
§ko@comp.tamu.edu
‖kjsun@tamu.edu
¶zhangzh275@mail.sysu.edu.cn

the observed enhancement of the α-particle yield is a consequence of its weaker Mott effect.

In the standard kinetic approach to heavy-ion collisions, such as the one based on the Boltzmann–Uehling-Uhlenbeck equation [21,22], there is a truncation at two-particle scatterings and also only the nucleonic degrees of freedom are considered. To include light nuclei in the kinetic approach, one can resort to the real-time Green's function formalism [20], in which a light nucleus consisting of A nucleons appears as a pole of the A-particle Green's function. The kinetic equations for light nuclei can then be derived by applying the Dyson equation in the vicinity of this pole [13]. Including all light nuclei with $A \leqslant 4$, we obtain the following coupled kinetic equations for the time evolution of their Wigner functions or phase-space distributions $f_\tau(\vec{r}, \vec{p}, t)$,

$$(\partial_t + \vec{\nabla}_p \epsilon_\tau \cdot \vec{\nabla}_r - \vec{\nabla}_r \epsilon_\tau \cdot \vec{\nabla}_p) f_\tau = I_\tau^{\rm coll}[f_n, f_p, \ldots], \quad (1)$$

where τ represents n, p, d, t, h, and α, as well as the pion (π) and Δ resonance. In the above equation, $\epsilon_\tau[f_n, f_p, \ldots]$ is the single-particle energy of the particle species τ, and it is usually derived from a density functional. The collision integral $I_\tau^{\rm coll}$ consists of a gain term ($<$) and a loss term ($>$),

$$I_\tau^{\rm coll} = K_\tau^<[f_n, f_p, \ldots](1 \pm f_\tau) - K_\tau^>[f_n, f_p, \ldots] f_\tau, \quad (2)$$

where the plus and minus signs are for bosons and fermions, respectively. Both gain and loss terms contain contributions from various scattering channels, which can be obtained through the diagrammatic expansion of the many-particle Green's function [13]. For light nuclei, we include following nucleon-induced catalytic reactions, $NNN \leftrightarrow Nd$, $NNNN \leftrightarrow Nt(h)$, $NNNNN \leftrightarrow N\alpha$, $NNt(h) \leftrightarrow N\alpha$, and the two-body inelastic channel $N\alpha \leftrightarrow dt(h)$. For the loosely bound deuteron, we do not include its production and absorption from t, h, and α breakup channels and their reverse reactions (e.g., $N\alpha \leftrightarrow NNNd$). For example, the α-particle loss term $K_\alpha^> f_\alpha$ in Eq. (2) is expressed as

$$\begin{aligned} K_\alpha^> f_\alpha = & \frac{\mathcal{S}_{5'} f_\alpha}{2E_\alpha} \int \prod_{i=1'}^{5'} \frac{d\vec{p}_i}{(2\pi\hbar)^3 2E_i} \frac{d\vec{p}_N}{(2\pi\hbar)^3 2E_N} \overline{|\mathcal{M}_{N\alpha\to NNNNN}|^2} g_N f_N \prod_{i=1'}^{5'} (1 \pm f_i)(2\pi)^4 \delta^4\left(\sum_{i=1'}^{5'} p_i - p_N - p_\alpha\right) \\ & + \frac{\mathcal{S}_{3'} f_\alpha}{2E_\alpha} \int \prod_{i=1'}^{3'} \frac{d\vec{p}_i}{(2\pi\hbar)^3 2E_i} \frac{d\vec{p}_N}{(2\pi\hbar)^3 2E_N} \overline{|\mathcal{M}_{N\alpha\to NNt}|^2} g_N f_N \prod_{i=1'}^{3'} (1 \pm f_i)(2\pi)^4 \delta^4\left(\sum_{i=1'}^{3'} p_i - p_N - p_\alpha\right) + t \to h \\ & + \frac{\mathcal{S}_{2'} f_\alpha}{2E_\alpha} \int \prod_{i=1'}^{2'} \frac{d\vec{p}_i}{(2\pi\hbar)^3 2E_i} \frac{d\vec{p}_N}{(2\pi\hbar)^3 2E_N} \overline{|\mathcal{M}_{N\alpha\to dt}|^2} g_N f_N \prod_{i=1'}^{2'} (1 \pm f_i)(2\pi)^4 \delta^4\left(\sum_{i=1'}^{2'} p_i - p_N - p_\alpha\right) + t \to h. \end{aligned} \quad (3)$$

In the above, $1'$–$5'$ denote final-state particles, and $\mathcal{S}_{5'}$, $\mathcal{S}_{3'}$, and $\mathcal{S}_{2'}$ are symmetry factors that take into account possible identical particles in the final state of a reaction.

The transition amplitudes in the kinetic equations can be deduced from the experimental differential cross sections for the loss term and the detailed balance relations for the gain term. For catalytic reactions, this can be achieved using the impulse approximation. Under this approximation, the spin-averaged squared transition matrix element of a catalytic reaction is decomposed into the product of the internal momentum-space wave function of the light nucleus and the spin-averaged squared amplitude of the nucleon-nucleon elastic-scattering amplitude $\overline{|M_{NN\to NN}|^2}$. As an example, the spin-averaged squared transition matrix element $\overline{|\mathcal{M}_{N\alpha\to NNNNN}|^2}$ for the reaction $N\alpha \to NNNNN$ can be approximately written as

$$\begin{aligned} & \overline{|\mathcal{M}_{N\alpha\to NNNNN}|^2} \\ & \quad \approx F(\sqrt{s}) \sum_{\substack{\text{spectator}\\ \text{nucleons}}} |\langle \vec{k}\vec{k}_\lambda\vec{k}_\mu|\phi_\alpha\rangle|^2 \overline{|M_{NN\to NN}|^2}, \end{aligned} \quad (4)$$

where $\vec{k}$, $\vec{k}_\lambda$, and $\vec{k}_\mu$ denote the three relative momenta between the constituent nucleons of the α particle. In the above, the summation runs over all combinations of spectator nucleons. For simplicity, the internal wave functions of light nuclei are chosen to have a Gaussian form in the present study.

Since the cross section obtained from the factor $\sum_{\substack{\text{spectator}\\ \text{nucleons}}} |\langle \vec{k}\vec{k}_\lambda\vec{k}_\mu|\phi_\alpha\rangle|^2 \overline{|M_{NN\to NN}|^2}$ in Eq. (4) for the reaction $N\alpha \to NNNNN$ may not agree with the measured one because of the possible inadequacy of the impulse approximation, a center-of-mass scattering energy $\sqrt{s}$-dependent factor $F(\sqrt{s})$ is introduced in Eq. (4) to account for these effects. $F(\sqrt{s})$ can be determined from comparing the nucleon-nucleus scattering cross sections from the impulse approximation with those measured from experiments. Because the nucleon-nucleus scattering at large incident energies is dominated by inelastic breakup reactions, we also require that the factor $F(\sqrt{s})$ or, more generally, the sum of $F(\sqrt{s})$ when there are many different outgoing channels, should approach 1.0 as $\sqrt{s}$ increases.

We show in Fig. 1 by dashed lines the cross sections of these breakup reactions used in the present kinetic approach, obtained by parametrizing the factor $F(\sqrt{s})$ for different nucleon-nucleus scatterings to reproduce the corresponding cross sections measured in experiments. Figures 1(a) and 1(b) show, respectively, the breakup cross sections of pd and ph. For the breakup of $p\alpha$, there are three different final-state channels of dh, $ppt(pnh)$, and $pppnn$. The $p\alpha \to dh$ channel is included to account for the cross section below the

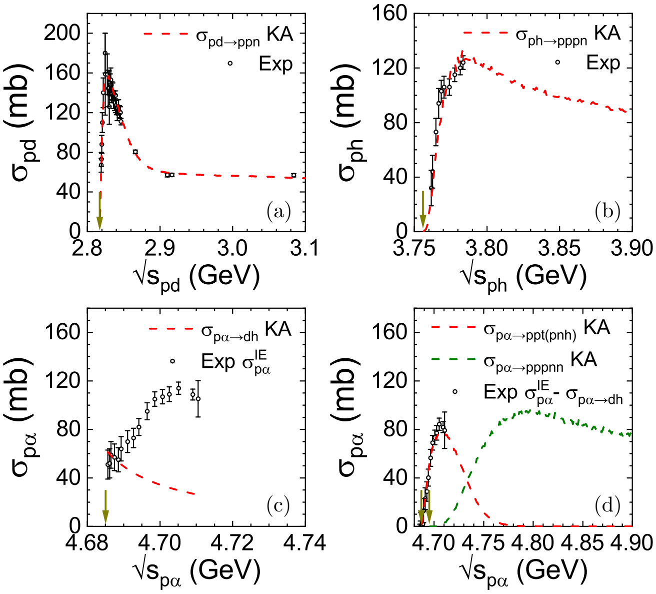

FIG. 1. Cross sections of inelastic (a) pd, (b) ph, (c) $p\alpha \rightarrow dh$, and (d) $p\alpha \rightarrow ppt(pnh)$ and $p\alpha \rightarrow pppnn$ from the impulse approximation (dashed lines) used in the present kinetic approach (KA). The measured cross sections (open circles) are taken from Refs. [23,24] and references therein, with $\sigma_{p\alpha}^{IE}$ in panel (c) being the measured inelastic $p\alpha$ cross section and after being subtracted by $\sigma_{p\alpha\rightarrow dh}$ in panel (d). The arrows denote the threshold of these reactions.

$p\alpha \rightarrow ppt(pnh)$ threshold, whose cross section is shown in Fig. 1(c). The cross section $\sigma_{p\alpha\rightarrow dh}$ is deduced from the measured cross section of the reaction $dt \rightarrow n\alpha$ [25] using the detailed balance relation. Apart from $p\alpha \rightarrow dh$, the total inelastic $p\alpha$ cross section is largely exhausted by $p\alpha \rightarrow ppt(pnh)$ at small $\sqrt{s_{p\alpha}}$ [red line in Fig. 1(d)] and by $p\alpha \rightarrow pppnn$ at large $\sqrt{s_{p\alpha}}$ [olive line in Fig. 1(d)]. The above assumption for the branching ratios of inelastic $p\alpha$ scattering is based on the argument that a proton with higher incident energy makes it easier for the α particle to fully breakup.

One of the important features of light nuclei in a nuclear medium is the Mott effect on their binding energies; i.e., they will no longer be bound if the phase-space density of their surrounding nucleons is too large. To include the Mott effect on a light nucleus, one should, in principle, solve an in-medium Schrödinger equation, which takes into account the Pauli-blocking effect, for the light nucleus moving with a momentum $\vec{P}$ in the nuclear medium. Because of the Pauli blocking of the constituent nucleons in the light nucleus due to the nucleons in nuclear medium, the resulting binding energy $E_B(\vec{P})$ is expected to decrease with increasing nucleon phase-space density in the nuclear medium. For a sufficiently large nucleon phase-space density around the light nucleus in the nuclear medium, $E_B(\vec{P})$ would vanish, and the light nucleus would no longer be bound. This criterion for the existence of light nuclei can be effectively implemented in the kinetic approach by introducing a phase-space cutoff in the collision integral for their production. Specifically, A free nucleons of

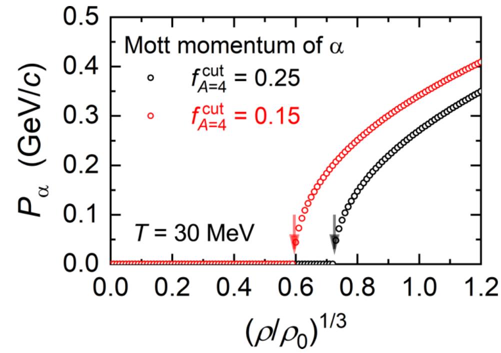

FIG. 2. Density dependence of the Mott momentum of the α-particle in nuclear matter at temperature $T = 30$ MeV, with $\rho_0 = 0.16\ \text{fm}^{-3}$ denoting the normal nuclear matter density. The arrows represent their corresponding Mott densities. The results are obtained with $f_{A=4}^{\text{cut}} = 0.25$ or 0.15.

total momentum $\vec{P}$ in a nuclear medium are allowed to form a nucleus of mass number A only if the average nucleon phase-space density of the medium around the light nucleus is less than a cutoff parameter f_A^{cut} [13], i.e.,

$$\langle f_N \rangle_A \equiv \int f_N\left(\frac{\vec{P}}{A} + \vec{p}\right)\rho_A(\vec{p})d\vec{p} \leqslant f_A^{\text{cut}}, \tag{5}$$

where $\rho_A(\vec{p})$ denotes the nucleon momentum distribution inside the light nucleus (related to its internal wave function), and f_N is the nucleon phase-space distribution in the medium.

For nuclear matter in thermal equilibrium with f_N given by the Fermi distribution, $E_B(\vec{P})$ decreases with decreasing $|\vec{P}|$ and vanishes below a critical momentum called the Mott momentum P_{Mott}. It has been shown that the density dependence of P_{Mott} obtained from Eq. (5) at a given temperature T for deuterons and tritons are consistent with those from the t-matrix approach [15], and the preferred value of f_A^{cut} shows little temperature dependence [15]. In Fig. 2, we show the density dependence of the Mott momentum of the α particle obtained for two different values of 0.25 and 0.15 for $f_{A=4}^{\text{cut}}$ in nuclear matter at $T = 30$ MeV, which is the typical temperature reached in intermediate-energy heavy-ion collisions. The Mott density of a light nucleus is then given by the maximum density at which a light nucleus of zero momentum can still be bound, as indicated by the arrows in the figure for the α particle. Its value for $f_{A=4}^{\text{cut}} = 0.25$ is around $0.4\rho_0$, which is significantly larger than that obtained in Refs. [26–28]. However, since most light nuclei in intermediate-energy heavy-ion collisions are produced and freeze-out chemically at high densities, only the Mott momentum for high density nuclear matter is relevant in our study. The Mott density shown in Fig. 2 is an extrapolation of the criterion in Eq. (5) to low densities and thus may not be directly compared to those given in Refs. [26–28]. Our obtained larger Mott density compared with previous theoretical calculations calls for further studies on the density dependence of the Mott momentum. We further note that the cutoff parameters $f_{A=2}^{\text{cut}}$, $f_{A=3}^{\text{cut}}$, and $f_{A=4}^{\text{cut}}$ can be considered as a surrogate for the strength of the Mott effects on the deuteron, triton or helium-3, and α particle, respectively. A smaller f_A^{cut} corresponds to a stronger Mott effect

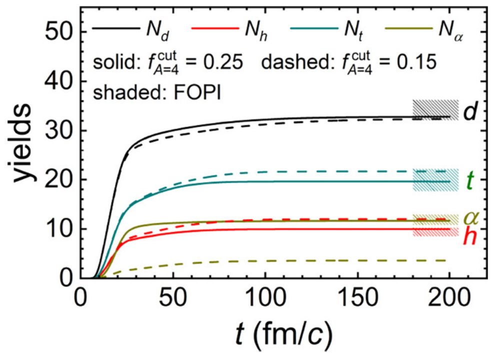

FIG. 3. Light-nuclei yields as functions of elapsed collision time in central Au + Au collisions at 0.4A GeV from the kinetic approach with $f^{\rm cut}_{A=2} = 0.11$, $f^{\rm cut}_{A=3} = 0.16$, and two different $f^{\rm cut}_{A=4} = 0.25$ and 0.15. The shaded areas represent the data measured by the FOPI Collaboration [16].

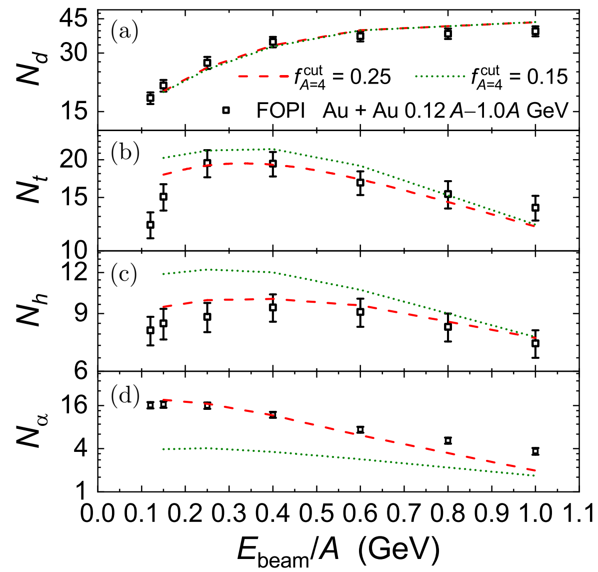

FIG. 4. Incident-energy dependence of light-nuclei yields from the kinetic approach with $f^{\rm cut}_{A=2} = 0.11$, $f^{\rm cut}_{A=3} = 0.16$, and $f^{\rm cut}_{A=4} = 0.25$. The results for a smaller $f^{\rm cut}_{A=4} = 0.15$ are also included for comparison. The experimental data are from the FOPI Collaboration [16].

and a larger $P_{\rm Mott}$. For the implications of the values of $f^{\rm cut}_A$ on the in-medium properties of light nuclei in nuclear matter, we leave them to a future study, and in the present study we treat them only as parameters for reproducing measured yields of light nuclei in intermediate-energy heavy-ion collisions.

We solve the kinetic equations by employing the test-particle ansatz [29], which approximates f_τ in terms of a large number of δ functions, i.e., $f_\tau(\vec{r}, \vec{p}) \approx \frac{(2\pi\hbar)^3}{g_\tau N_E} \sum_{i=1}^{N_\tau N_E} \delta(\vec{r}_i - \vec{r})\delta(\vec{p}_i - \vec{p})$, where g_τ and N_E denote, respectively, the spin degeneracy of particle species τ and the number of test particles or ensembles used in solving the kinetic equations. To ensure the convergence of numerical results, a sufficiently large N_E is used. To improve the numerical accuracy, we further adopt the lattice Hamiltonian method [30,31] to treat the drift terms on the left-hand side of Eq. (1). As to the single-particle energy ϵ_τ in Eq. (1), we use the one derived from the Skyrme pseudopotential [32,33]. For the collision integral on the right-hand side of Eq. (1), it is treated by the stochastic method [13,34], in which the scattering probability of initial-state particles within a time interval is calculated directly from the loss term $K^>_\tau f_\tau$.

In the present study, we apply the above kinetic approach to central Au + Au collisions at the incident energy from $E_{\rm beam} = 0.25A$ GeV to 1.0A GeV. Besides elastic scatterings and the many-body scatterings related to light-nuclei production and dissociation, we include in the kinetic approach also scatterings related to Δ resonances and pions, i.e., $NN \leftrightarrow N\Delta$ and $\Delta \leftrightarrow N\pi$ [35]. Since in heavy-ion collisions in this energy region, nucleons still dominate over pions, we neglect the production and dissociation of light nuclei with the pion as the catalyzer [36,37].

We first show in Fig. 3 the time evolution of light-nuclei yields in central Au + Au collisions at 0.4A GeV from our kinetic approach, with $f^{\rm cut}_{A=2} = 0.11$ for the deuteron, $f^{\rm cut}_{A=3} = 0.16$ for the triton and helium-3, and two different $f^{\rm cut}_{A=4} = 0.25$ and 0.15 for the α particle. It is seen that decreasing $f^{\rm cut}_{A=4}$ significantly reduces the α-particle yield. We also notice from the figure that the number of light nuclei increases significantly in the early phase of the time evolution, which corresponds to the compressing stage of the collision, because of the enhanced production rate of light nuclei in dense nuclear matter. Since light nuclei are abundantly produced during the early compression stage of intermediate-energy heavy-ion collisions, it is important to include them dynamically throughout the collisions, rather than to introduce them merely at the kinetic freeze-out of the collisions like in the coalescence model.

In Fig. 4, we show the beam-energy dependence of light-nuclei yields in central Au+Au collisions from the kinetic approach. They are obtained with the Mott effect of light nuclei properly incorporated by choosing appropriate values for the cutoff parameters $f^{\rm cut}_A$. Due to the tight binding of the α particle in free space, it is more difficult for the α particle to dissolve in nuclear medium than it is for the deuteron, the triton, and helium-3, resulting in a weaker Mott effect and a smaller $P_{\rm Mott}/A$ for the α particle in nuclear medium. This is the same argument used in the calculation of the properties of nuclear matter with light nuclei from the quantum statistical approach and the generalized relativistic mean-field model [28,38]. It is also consistent with the larger Mott density of the α particle than the Mott densities of the deuteron, triton and helium-3 deduced from experiments [9]. This explains the larger value we have used for $f^{\rm cut}_{A=4}$ than the values for $f^{\rm cut}_{A=2}$ and $f^{\rm cut}_{A=3}$.

It is seen in Fig. 4 that the present kinetic approach with $f^{\rm cut}_{A=2} = 0.11$, $f^{\rm cut}_{A=3} = 0.16$, and $f^{\rm cut}_{A=4} = 0.25$ reproduces reasonably the measured light-nuclei yields in central Au + Au collisions [16] for a wide range of incident energies, especially for the large α-particle yield at lower incident energies. At these energies, the measured yield of the α particle surpasses that of helium-3, which is in sharp contrast to the prediction from the thermal model, which gives a decreasing yield with an increasing mass number of light nuclei. If we had used a smaller $f^{\rm cut}_{A=4} = 0.15$ (while fixing $f^{\rm cut}_{A=2}$ and $f^{\rm cut}_{A=3}$), which corresponds to a stronger Mott effect and a larger Mott momentum for the α particle, the α-particle yield would be significantly smaller as shown in Fig. 4(d). Our result thus indicates that the observed enhancement of the α-particle yield in lower-energy collisions can be attributed to a weaker Mott effect on the α particle than that on the deuteron, triton and helium-3, as a result of its much larger binding energy.

In summary, to provide a dynamical description of light-nuclei production in intermediate-energy heavy-ion collisions, we have included the light-nuclei degrees of freedom with $A \leqslant 4$ in the kinetic approach. The breakup of light nuclei by nucleons and their reverse reactions are included to account for the conversion between nucleons and light-nuclei during the collisions. The Mott effects of light nuclei are also included by considering the nucleon phase-space density $\langle f_N \rangle$ around them, and a light nucleus can exist only if $\langle f_N \rangle$ is less than the cutoff parameter $f^{\rm cut}_A$. With appropriate values of $f^{\rm cut}_A$ for different species of light nuclei, the present kinetic approach has reasonably reproduced the yields of light nuclei in central Au + Au collisions at incident energies from 0.25A GeV to 1.0A GeV measured by the FOPI Collaboration. Our study has clearly demonstrated that the observed enhancement of the α-particle yield compared with that of helium-3 at low incident energies is a consequence of the Mott effect of light nuclei. Therefore, studying the light-nuclei yields in intermediate-energy heavy-ion collisions allows one to determine the cutoff parameters $f^{\rm cut}_A$ and thus the strength of their Mott effect. The implications of the preferred values of $f^{\rm cut}$ obtained in this work on the medium properties of light nuclei in warm nuclear matter will be reported in a forthcoming study.

The present kinetic approach can be further used to study phenomena related to light nuclei in nuclear reactions, such as the iso-scaling in intermediate-energy heavy-ion collisions [39] and the effect of the α clusters formed on the surface of heavy nuclei [40], as well as the role of light nuclei in core-collapse supernovas, compact stars, and their mergers [11,12]. Since the nuclear matter produced in heavy-ion collisions around the Fermi energy could undergo the spinodal transition [41–45], which would lead to the production of heavy fragments with mass number $A \geqslant 5$, to describe the dynamics of these heavy fragments requires the extension of the standard kinetic approach, as used in the present study, to include the fluctuations of nucleon phase-space distributions or Wigner functions [46]. A possible and worthwhile further development of the present approach is to include such fluctuations in the kinetic approach, so that low-energy nuclear reactions can also be properly described. These studies will be pursued in the future.

We thank C. Zhong for setting up and maintaining the GPU server. This work was supported in part by the National Natural Science Foundation of China under Contracts No. 11890714, No. 12147101, No. 12235010, No. 11625521, and No. 12375121; the National Key Research and Development Program of China under Grants No. 2018YFE0104600 and No. 2022YFA1602303; the National SKA Program of China No. 2020SKA0120300; the Guangdong Major Project of Basic and Applied Basic Research No. 2020B0301030008; and the U.S. Department of Energy under Award No. DE-SC0015266.

[1] V. Baran, M. Colonna, V. Greco, and M. Di Toro, Reaction dynamics with exotic nuclei, Phys. Rep. **410**, 335 (2005).
[2] B.-A. Li, L.-W. Chen, and C. M. Ko, Recent progress and new challenges in isospin physics with heavy-ion reactions, Phys. Rep. **464**, 113 (2008).
[3] P. Danielewicz, R. Lacey, and W. G. Lynch, Determination of the equation of state of dense matter, Science **298**, 1592 (2002).
[4] M. A. Famiano, T. Liu, W. G. Lynch, M. Mocko, A. M. Rogers, M. B. Tsang, M. S. Wallace, R. J. Charity, S. Komarov, D. G. Sarantites, L. G. Sobotka, and G. Verde, Neutron and Proton Transverse Emission Ratio Measurements and the Density Dependence of the Asymmetry Term of the Nuclear Equation of State, Phys. Rev. Lett. **97**, 052701 (2006).
[5] Z. Xiao, B.-A. Li, L.-W. Chen, G.-C. Yong, and M. Zhang, Circumstantial Evidence for a Soft Nuclear Symmetry Energy at Suprasaturation Densities, Phys. Rev. Lett. **102**, 062502 (2009).
[6] J. Estee *et al.* (SπRIT Collaboration), Probing the Symmetry Energy with the Spectral Pion Ratio, Phys. Rev. Lett. **126**, 162701 (2021).
[7] A. Ono, Dynamics of clusters and fragments in heavy-ion collisions, Prog. Part. Nucl. Phys. **105**, 139 (2019).
[8] L. Qin, K. Hagel, R. Wada, J. B. Natowitz, S. Shlomo, A. Bonasera, G. Röpke, S. Typel, Z. Chen, M. Huang, J. Wang, H. Zheng, S. Kowalski, M. Barbui, M. R. D. Rodrigues, K. Schmidt, D. Fabris, M. Lunardon, S. Moretto, G. Nebbia *et al.*, Laboratory Tests of Low Density Astrophysical Nuclear Equations of State, Phys. Rev. Lett. **108**, 172701 (2012).
[9] K. Hagel, R. Wada, L. Qin, J. B. Natowitz, S. Shlomo, A. Bonasera, G. Röpke, S. Typel, Z. Chen, M. Huang, J. Wang, H. Zheng, S. Kowalski, C. Bottosso, M. Barbui, M. R. D. Rodrigues, K. Schmidt, D. Fabris, M. Lunardon, S. Moretto *et al.*, Experimental Determination of In-Medium Cluster Binding Energies and Mott Points in Nuclear Matter, Phys. Rev. Lett. **108**, 062702 (2012).
[10] H. Pais, R. Bougault, F. Gulminelli, C. Providência, E. Bonnet, B. Borderie, A. Chbihi, J. D. Frankland, E. Galichet, D. Gruyer, M. Henri, N. Le Neindre, O. Lopez, L. Manduci, M. Parlôg, and G. Verde, Low Density In-Medium Effects on Light Clusters from Heavy-Ion Data, Phys. Rev. Lett. **125**, 012701 (2020).
[11] K. Sumiyoshi and G. Röpke, Appearance of light clusters in post-bounce evolution of core-collapse supernovae, Phys. Rev. C **77**, 055804 (2008).
[12] M. Oertel, M. Hempel, T. Klähn, and S. Typel, Equations of state for supernovae and compact stars, Rev. Mod. Phys. **89**, 015007 (2017).
[13] P. Danielewicz and G. F. Bertsch, Production of deuterons and pions in a transport model of energetic heavy-ion reactions, Nucl. Phys. A **533**, 712 (1991).

[14] P. Danielewicz and Q. Pan, Blast of light fragments from central heavy-ion collisions, Phys. Rev. C **46**, 2002 (1992).

[15] C. Kuhrts, M. Beyer, P. Danielewicz, and G. Röpke, Medium corrections in the formation of light charged particles in heavy ion reactions, Phys. Rev. C **63**, 034605 (2001).

[16] FOPI Collaboration, Systematics of central heavy ion collisions in the 1*A* GeV regime, Nucl. Phys. A **848**, 366 (2010).

[17] R. Bougault, B. Borderie, A. Chbihi, Q. Fable, J. D. Frankland, E. Galichet, T. Genard, D. Gruyer, M. Henri, M. La Commara, N. Le Neindre, I. Lombardo, O. Lopez, M. Pârlog, P. Pawłowski, G. Verde, E. Vient, and M. Vigilante, Light cluster production in central symmetric heavy-ion reactions from Fermi to Gev energies, Symmetry **13**, 1406 (2021).

[18] G. Röpke, L. Münchow, and H. Schulz, Particle clustering and Mott transitions in nuclear matter at finite temperature: (I). Method and general aspects, Nucl. Phys. A **379**, 536 (1982).

[19] G. Röpke, M. Schmidt, L. Münchow, and H. Schulz, Particle clustering and Mott transition in nuclear matter at finite temperature: (II). Self-consistent ladder Hartree-Fock approximation and model calculations for cluster abundances and the phase diagram, Nucl. Phys. A **399**, 587 (1983).

[20] J. Rammer, *Quantam Field Theory of Non-Equilibrium States* (Cambridge University, Cambridge, England, 2007).

[21] G. F. Bertsch and S. Das Gupta, A guide to microscopic models for intermediate energy heavy ion collisions, Phys. Rep. **160**, 189 (1988).

[22] TEMP Collaboration, Transport model comparison studies of intermediate-energy heavy-ion collisions, Prog. Part. Nucl. Phys. **125**, 103962 (2022).

[23] R. F. Carlson, P. Doherty, D. J. Margaziotis, I. Slaus, S. Y. Tin, and W. T. H. van Oers, Proton-deuteron total reaction cross-sections in the energy range (20÷50) MeV, Lett. Nuovo Cimento **8**, 319 (1973).

[24] A. M. Sourkes, A. Houdayer, W. T. H. van Oers, R. F. Carlson, and R. E. Brown, Total reaction cross section for protons on ^{3}He and ^{4}He between 18 and 48 MeV, Phys. Rev. C **13**, 451 (1976).

[25] S. J. Bame and J. E. Perry, T(d,n)He^4 Reaction, Phys. Rev. **107**, 1616 (1957).

[26] G. Röpke, A. Schnell, P. Schuck, and P. Nozières, Four-Particle Condensate in Strongly Coupled Fermion Systems, Phys. Rev. Lett. **80**, 3177 (1998).

[27] T. Sogo, G. Röpke, and P. Schuck, Critical temperature for α-particle condensation in asymmetric nuclear matter, Phys. Rev. C **82**, 034322 (2010).

[28] S. Typel, G. Röpke, T. Klähn, D. Blaschke, and H. H. Wolter, Composition and thermodynamics of nuclear matter with light clusters, Phys. Rev. C **81**, 015803 (2010).

[29] C.-Y. Wong, Dynamics of nuclear fluid. VIII. Time-dependent Hartree-Fock approximation from a classical point of view, Phys. Rev. C **25**, 1460 (1982).

[30] R. J. Lenk and V. R. Pandharipande, Nuclear mean field dynamics in the lattice Hamiltonian Vlasov method, Phys. Rev. C **39**, 2242 (1989).

[31] R. Wang, Lie-Wen Chen, and Z. Zhang, Nuclear collective dynamics in the lattice Hamiltonian Vlasov method, Phys. Rev. C **99**, 044609 (2019).

[32] F. Raimondi, B. G. Carlsson, and J. Dobaczewski, Effective pseudopotential for energy density functionals with higher-order derivatives, Phys. Rev. C **83**, 054311 (2011).

[33] R. Wang, L.-W. Chen, and Y. Zhou, Extended Skyrme interactions for transport model simulations of heavy-ion collisions, Phys. Rev. C **98**, 054618 (2018).

[34] R. Wang, Z. Zhang, L.-W. Chen, C. M. Ko, and Y.-G. Ma, Constraining the in-medium nucleon-nucleon cross section from the width of nuclear giant dipole resonance, Phys. Lett. B **807**, 135532 (2020).

[35] A. Ono, J. Xu, M. Colonna, P. Danielewicz, C. M. Ko, M. B. Tsang, Y.-J. Wang, H. Wolter, Y.-X. Zhang, L.-W. Chen, D. Cozma, H. Elfner, Z.-Q. Feng, N. Ikeno, B.-A. Li, S. Mallik, Y. Nara, T. Ogawa, A. Ohnishi, D. Oliinychenko *et al.*, Comparison of heavy-ion transport simulations: Collision integral with pions and Δ resonances in a box, Phys. Rev. C **100**, 044617 (2019).

[36] D. Oliinychenko, L.-G. Pang, H. Elfner, and V. Koch, Microscopic study of deuteron production in PbPb collisions at $\sqrt{s} = 2.76$ TeV via hydrodynamics and a hadronic afterburner, Phys. Rev. C **99**, 044907 (2019).

[37] K.-J. Sun, R. Wang, C. M. Ko, Y.-G. Ma, and C. Shen, Unveiling the dynamics of nucleosynthesis in relativistic heavy-ion collisions, arXiv:2207.12532.

[38] Z.-W. Zhang and L.-W. Chen, Low density nuclear matter with light clusters in a generalized nonlinear relativistic mean-field model, Phys. Rev. C **95**, 064330 (2017).

[39] The SπRIT Collaboration, Isoscaling in central Sn+Sn collisions at 270 MeV/u, Eur. Phys. J. A **58**, 201 (2022).

[40] J. Tanaka, Z. Yang, S. Typel, S. Adachi, S. Bai, P. van Beek, D. Beaumel, Y. Fujikawa, J. Han, S. Heil, S. Huang, A. Inoue, Y. Jiang, M. Knösel, N. Kobayashi, Y. Kubota, W. Liu, J. Lou, Y. Maeda, Y. Matsuda *et al.*, Formation of α clusters in dilute neutron-rich matter, Science **371**, 260 (2021).

[41] B. Borderie *et al.* (INDRA Collaboration), Evidence for Spinodal Decomposition in Nuclear Multifragmentation, Phys. Rev. Lett. **86**, 3252 (2001).

[42] P. Chomaz, M. Colonna, and J. Randrup, Nuclear spinodal fragmentation, Phys. Rep. **389**, 263 (2004).

[43] R. Wang, Y.-G. Ma, R. Wada, L.-W. Chen, W.-B. He, H.-L. Liu, and K.-J. Sun, Nuclear liquid-gas phase transition with machine learning, Phys. Rev. Res. **2**, 043202 (2020).

[44] C. Liu, X.-G. Deng, and Y.-G. Ma, Density fluctuations in intermediate-energy heavy-ion collisions, Nucl. Sci. Tech. **33**, 52 (2022).

[45] B. Borderie, N. Le Neindre, M. F. Rivet, P. Désesquelles, E. Bonnet, R. Bougault, A. Chbihi, D. Dell'Aquila, Q. Fable, J. D. Frankland, E. Galichet, D. Gruyer, D. Guinet, M. La Commara, I. Lombardo, O. Lopez, L. Manduci, P. Napolitani, M. Pârlog, E. Rosato *et al.*, Phase transition dynamics for hot nuclei, Phys. Lett. B **782**, 291 (2018).

[46] M. Colonna, M. Di Toro, A. Guarnera, S. Maccarone, M. Zielinska-Pfabé, and H. H. Wolter, Fluctuations and dynamical instabilities in heavy-ion reactions, Nucl. Phys. A **642**, 449 (1998).